CHEMISTRY
A EUROPEAN JOURNAL

Synthetic and Theoretical Study of the Incorporation of Metal Halides in $[\{Ti(\eta^5\text{-}C_5Me_5)(\mu\text{-}NH)\}_3(\mu_3\text{-}N)]$

María García-Castro,[a] José Gracia,[b] Avelino Martín,[a] Miguel Mena,*[a] Josep-M. Poblet,[b] José Pedro Sarasa,[c] and Carlos Yélamos[a]

Abstract: The capacity of the imido-nitrido organometallic ligand $[\{Ti(\eta^5\text{-}C_5Me_5)(\mu\text{-}NH)\}_3(\mu_3\text{-}N)]$ (**1**) to entrap main group metal halides MX_n has been investigated. Treatment of **1** with metal halides in toluene or dichloromethane afforded several soluble adducts $[MX_n(L)]$ (L = **1**) in good yields. The reaction of **1** with one equivalent of Group 1 and 13 monohalides MX afforded single cube-type complexes $[XM\{(\mu_3\text{-}NH)_3Ti_3(\eta^5\text{-}C_5Me_5)_3(\mu_3\text{-}N)\}]$ (M = Li, X = Br (**2**), I (**3**); M = Na, X = I (**4**); M = In, X = I (**5**); M = Tl, X = I (**6**)). Analogous treatment of **1** with Group 2 and 14 dihalides MX_2 gave the corresponding adducts $[I_2M\{(\mu_3\text{-}NH)_3Ti_3(\eta^5\text{-}C_5Me_5)_3(\mu_3\text{-}N)\}]$ (M = Mg (**7**), Ca (**8**), Sr (**9**)) and $[Cl_2M\{(\mu_3\text{-}NH)_3Ti_3(\eta^5\text{-}C_5Me_5)_3(\mu_3\text{-}N)\}]$ (M = Sn (**10**), Pb (**11**)). The treatment of **1** with SnI_2 or the reaction of **10** with MeI at 60 °C afforded two azametallocubane units linked by two bridging iodine atoms $[\{ISn(\mu_3\text{-}NH)_3Ti_3(\eta^5\text{-}C_5Me_5)_3(\mu_3\text{-}N)\}_2(\mu\text{-}I)_2]$ (**12**). Indium triiodide reacted with **1** in toluene to form the adduct $[I_3In(\mu_3\text{-}NH)_3Ti_3(\eta^5\text{-}C_5Me_5)_3(\mu_3\text{-}N)]$ (**13**). Density functional theory calculations have been carried out to study these processes and evaluate the influence of the solvent. X-ray crystal structure determinations have been performed for complexes **10**, **12**, and **13**.

Keywords: density functional calculations · halides · N ligands · nitrido complexes · titanium

Introduction

The titanium imido-nitrido complex $[\{Ti(\eta^5\text{-}C_5Me_5)(\mu\text{-}NH)\}_3(\mu_3\text{-}N)]$ (**1**)[1,2] is a useful reagent for the preparation of cube-type heterometallic nitrido complexes.[3,4,5,6,7,8,9] The structure determined for **1** shows an incomplete cube-type $[Ti_3N_4]$ core with three NH electron-donor imido groups in the base (Scheme 1). In our previous studies we have noted that **1** is capable of acting as a neutral polydentate ligand (**A**) to d^0, d^6, and d^8 transition-metal centers through the basal imido-nitrogen atoms.[3,4,6] These NH groups can be deprotonated if the coordination sphere of the incorporated metal contains imido, amido, or alkyl ligands, to give monoanionic (**B**), dianionic (**C**), and even trianionic (**D**) forms of **1**, along with the elimination of amine or alkane.[4,5,7,8,9]

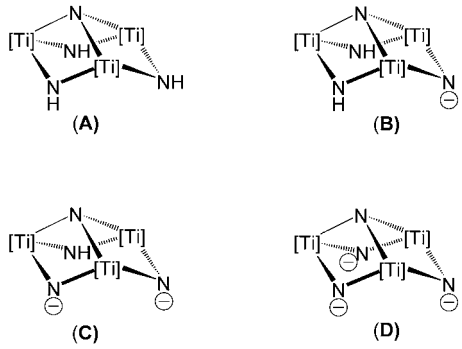

Scheme 1. Neutral and ionic forms of **1**. [Ti] = $Ti(\eta^5\text{-}C_5Me_5)$.

In these processes, the displacement of labile ligands by **1** is presumably the first and determining step in the preparation of cube-type derivatives.

In addition, we have recently demonstrated that **1** is able to break the polymeric chain structure of cyclopentadienide complexes of lithium, sodium, and thallium to give soluble

[a] M. García-Castro, Dr. A. Martín, Dr. M. Mena, Dr. C. Yélamos
Departamento de Química Inorgánica, Universidad de Alcalá
Campus Universitario, 28871 Alcalá de Henares-Madrid (Spain)
Fax: (+34) 918-854-683
E-mail: miguel.mena@uah.es

[b] Dr. J. Gracia, Prof. J.-M. Poblet
Department de Química Física i Inorgánica Universitat Rovira i Virgili
Imperial Tarraco 1, 43005 Tarragona (Spain)

[c] Dr. J. P. Sarasa
Departamento de Química Física y Química Orgánica
Universidad de Zaragoza. Ciudad Universitaria s/n, 50009 Zaragoza (Spain)

Supporting information for this article is available on the WWW under http://www.chemeurj.org/ or from the author.

DOI: 10.1002/chem.200400553

cube-type adducts $[(\eta^5\text{-}C_5H_5)M\{(\mu_3\text{-}NH)_3Ti_3(\eta^5\text{-}C_5Me_5)_3(\mu_3\text{-}N)\}]$.[10] In this way, a new goal for complex **1** could be the rupture of the highly stable metal halide lattices to yield molecular complexes. A literature search reveals many examples of entrapment of metal halides by ligands to yield molecular complexes.[11] However, most of the reported MX_n soluble adducts come from in situ generated molecules,[12] and there are very few examples of *direct* reactions of ligands with the metal halide lattices.[13,14]

Herein we describe the treatment of solid alkali, alkaline-earth, Group 13, and Group 14 metal halides in aromatic or halogenated solvents with **1**. Density functional theory (DFT) calculations have been carried out to study these processes and the influence of the solvent on the success of the reactions.

Results and Discussion

Coordination of $[\{Ti(\eta^5\text{-}C_5Me_5)(\mu\text{-}NH)\}_3(\mu_3\text{-}N)]$ to metal monohalides MX: The preparation of the adducts $[XM\{(\mu_3\text{-}NH)_3Ti_3(\eta^5\text{-}C_5Me_5)_3(\mu_3\text{-}N)\}]$ (M = Li, X = Br (**2**), I (**3**); M = Na, X = I (**4**); M = In, X = I (**5**), Tl, X = I (**6**)) is outlined in Scheme 2. Solutions of complexes **2**–**6** are obtained by addition of toluene or dichloromethane to a mixture of **1** and the anhydrous metal halides. After workup, the compounds were isolated in 48–70% yields as yellow or brown solids that are soluble in toluene or benzene, but scarcely soluble in n-hexane. Solutions of these complexes in [D_6]benzene remain unaltered over several months under an argon atmosphere.

Abstract in Spanish: *El ligando imido-nitruro $[\{Ti(\eta^5\text{-}C_5Me_5)(\mu\text{-}NH)\}_3(\mu_3\text{-}N)]$ (**1**) incorpora con facilidad diversos haluros metálicos de los grupos principales. Los procesos tienen lugar en tolueno o diclorometano a temperatura ambiente y permiten obtener con buenos rendimientos complejos nitruro tipo cubo. La reacción con monohaluros MX de los Grupos 1 y 13 da lugar a los derivados azaheterometalocubanos $[XM(\mu_3\text{-}NH)_3Ti_3(\eta^5\text{-}C_5Me_5)_3(\mu_3\text{-}N)]$ (M = Li, X = Br (**2**), I (**3**); M = Na, X = I (**4**); M = In, X = I (**5**); M = Tl, X = I (**6**)). En condiciones análogas, los dihaluros MX_2 de los Grupos 2 y 14 originan los aductos $[I_2M(\mu_3\text{-}NH)_3Ti_3(\eta^5\text{-}C_5Me_5)_3(\mu_3\text{-}N)]$ (M = Mg (**7**), Ca (**8**), Sr (**9**)) y $[Cl_2M\{(\mu_3\text{-}NH)_3Ti_3(\eta^5\text{-}C_5Me_5)_3(\mu_3\text{-}N)\}]$ (M = Sn (**10**), Pb (**11**)). La reacción de **1** con SnI_2 o el tratamiento de **10** con MeI a 60 °C conducen a la obtención de un complejo constituido por dos azametalocubanos unidos por un doble puente de iodo $[\{ISn(\mu_3\text{-}NH)_3Ti_3(\eta^5\text{-}C_5Me_5)_3(\mu_3\text{-}N)\}_2(\mu\text{-}I)_2]$ (**12**). La incorporación de triioduro de indio, en tolueno da el aducto $[I_3In(\mu_3\text{-}NH)_3Ti_3(\eta^5\text{-}C_5Me_5)_3(\mu_3\text{-}N)]$ (**13**). La Teoría del Funcional de la Densidad ha permitido abordar el estudio de estos procesos y evaluar el efecto del disolvente. Las estructuras de los complejos **10**, **12** y **13** se han determinado mediante difracción de rayos-X de monocristal.*

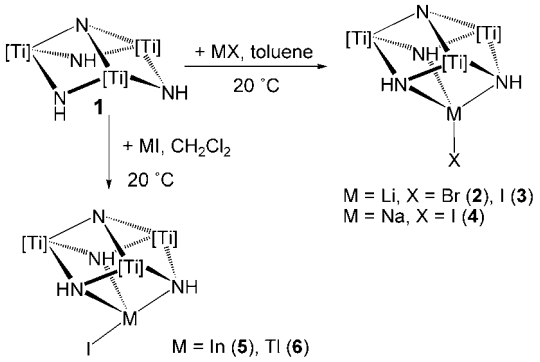

Scheme 2. Reaction of **1** with MX. [Ti] = $Ti(\eta^5\text{-}C_5Me_5)$.

However, LiCl, NaCl, NaBr, KBr, and KI did not react under the same conditions. Furthermore, we did not obtain the adduct $[ClLi(\mu_3\text{-}NH)_3Ti_3(\eta^5\text{-}C_5Me_5)_3(\mu_3\text{-}N)]$ even by generating LiCl and **1** in situ from the reaction of $[Li\{[(\mu_3\text{-}NH)_2(\mu_3\text{-}N)\{Ti_3(\eta^5\text{-}C_5Me_5)_3(\mu_3\text{-}N)\}]_2]$[5] and NEt_3HCl in toluene. Among the Group 13 metal halides MX (M = In, Tl), only the InI and TlI iodides afforded the stable adducts **5** and **6**, whereas TlCl did not react, and InCl gave the adduct $[ClIn\{(\mu_3\text{-}NH)_3Ti_3(\eta^5\text{-}C_5Me_5)_3(\mu_3\text{-}N)\}]$, which was characterized by NMR spectroscopy,[15] but could not be isolated in a pure form.

Complexes **2**–**6** were characterized by spectral and analytical techniques. The mass spectra obtained for **2** and **4** (EI, 70 eV) suggest a monomeric formulation in the gas phase. IR spectra (KBr) show one ν_{NH} vibration, between 3349 and 3337 cm^{-1}, for the alkali metal derivatives **2**–**4**, and two ν_{NH} vibrations, in the range 3352–3246 cm^{-1}, for complexes **5** and **6**. These ranges are similar to the value determined for **1**, 3352 cm^{-1},[2] and other azaheterometallocubane derivatives.[3–10] ^1H and $^{13}C\{^1H\}$ NMR spectra in [D_6]benzene at room temperature of **2**–**6** show resonances for equivalent NH and C_5Me_5 groups suggesting a highly symmetrical structure in solution. The NH resonance signals in these spectra (δ = 13.6–12.7 ppm) are shifted to higher field than that found for **1** (δ = 13.8 ppm). We have noted an analogous shift in several transition and main group azaheterometallocubane derivatives, and used those data to propose the coordination of the NH groups to the incorporated elements.[5,10] $^{13}C\{^1H\}$ NMR spectra revealed a singlet for the *ipso*-carbon resonance of the C_5Me_5 ligands (δ = 118–120 ppm), which is slightly shifted downfield with respect to that found for **1** (δ = 117.1 ppm).

Repeated attempts to obtain single crystals for X-ray crystallographic studies of complexes **2**–**6** were unsuccessful; therefore, DFT calculations were carried out to establish the structure for the model complexes $[XM\{(\mu_3\text{-}NH)_3Ti_3(\eta^5\text{-}C_5H_5)_3(\mu_3\text{-}N)\}]$ (M = Li, Na, K, Rb, Cs, In, Tl; X = F, Cl, Br, I). The optimized geometries under C_{3v} symmetry restrictions for the alkali metal complexes show distorted tetrahedral environments for the alkali-metal centers (see Figure 1), similar to those recently determined by X-ray crystallographic studies for the adducts $[(\eta^5\text{-}C_5H_5)Na\{(\mu_3\text{-}$

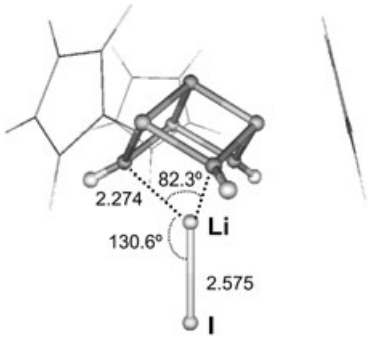

Figure 1. Computed geometry and selected parameters (distances [Å] and angles [°]) for $[ILi\{(\mu_3\text{-}NH)_3Ti_3(\eta^5\text{-}C_5H_5)_3(\mu_3\text{-}N)\}]$.

$NH)_3Ti_3(\eta^5\text{-}C_5Me_5)_3(\mu_3\text{-}N)\}]$[10] and $[MeSi(2\text{-}C_5H_4N)_3LiX]$ (X = 0.2 Br, 0.8 Cl).[16] Structures with C_s symmetry, in which the MX unit forms angles wider than 30° with the axis that crosses the tripodal ligand, were also computed for the LiBr, LiI, and NaI halides. In the three complexes, the C_s and C_{3v} geometries are almost degenerate.

In the case of the indium(I) and thallium(I) adducts, the metal center has a lone pair of electrons in the coordination sphere, which makes its electronic structure different. For these complexes, we have calculated geometries with C_{3v} symmetry, analogous to that found for the alkali-metal complexes, and two optimal C_s geometries, in which alternatively the iodine atom occupies one axial or one equatorial position of the pseudo-trigonal-bypiramidal center. The C_{3v} form is disfavored in these systems due to the presence of the metal lone pair. Thus, this symmetric form is higher in energy than the most stable C_s structure by 36 kJ mol^{-1} for the indium(I) derivative (Scheme 3). For both indium and thallium complexes, the C_s structure with the lone pair occupying one equatorial position is the most stable, but the energy difference between the two C_s isomers is quite small (3.1 kJ mol^{-1} for $[IIn\{(\mu_3\text{-}NH)Ti_3(\eta^5\text{-}C_5H_5)_3(\mu\text{-}NH)_2(\mu_3\text{-}N)\}]$). In fact, the analogous recently reported thallium cyclopentadienide adduct $[(\eta^5\text{-}C_5H_5)Tl\{(\mu_3\text{-}NH)_3Ti_3(\eta^5\text{-}C_5Me_5)_3(\mu_3\text{-}N)\}]$ shows a distorted trigonal-bypiramidal geometry around the thallium(I) center in which the lone pair occupies the axial position.[10]

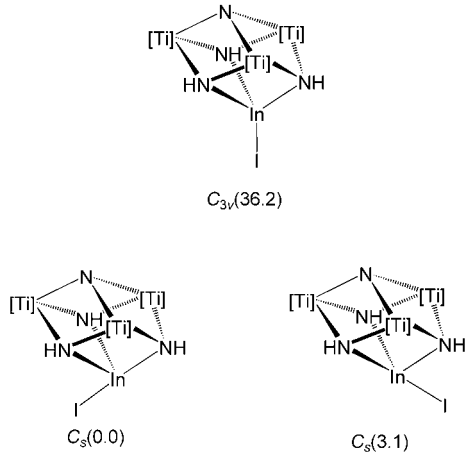

Scheme 3. Calculated geometries and relative energy values (kJ·mol^{-1}) for the $[IIn\{(\mu_3\text{-}NH)_3Ti_3(\eta^5\text{-}C_5H_5)_3(\mu_3\text{-}N)\}]$ complex.

Importantly, the C_{3v} structure is not the transition state between the two C_s isomers in Scheme 3, since this path is expected to occur by rotation around the vertical axis, with a low energy barrier, which could justify the behavior of these complexes in the NMR spectra.

Coordination of $[\{Ti(\eta^5\text{-}C_5Me_5)(\mu\text{-}NH)\}_3(\mu_3\text{-}N)]$ to metal dihalides MX_2: The synthetic chemistry of adducts formed from **1** and metal dihalides is outlined in Scheme 4. Adducts

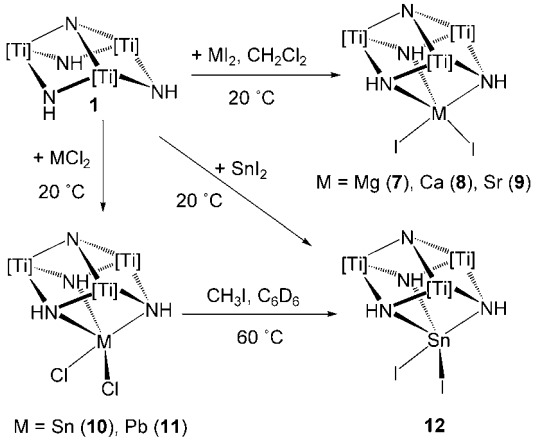

Scheme 4. Reaction of **1** with MX_2. [Ti] = Ti(η^5-C_5Me_5).

of alkaline-earth metal halides were obtained by treatment of the metal diiodides MI_2 (M = Mg, Ca, Sr) with **1** ($\geq$1 equiv) in dichloromethane at room temperature. The slight excess of **1** is crucial to ensure the complete reaction of the metal halides in dichloromethane, and can be eliminated later by washing the solids with toluene. In this way, the adducts $[I_2M\{(\mu_3\text{-}NH)_3Ti_3(\eta^5\text{-}C_5Me_5)_3(\mu_3\text{-}N)\}]$ (M = Mg (**7**); M = Ca (**8**); M = Sr (**9**)) were isolated in 55–89 % yields as yellow solids, which are moderately soluble in dichloromethane or chloroform, but scarcely soluble in arene solvents.

The analogous reaction with tin(II) and lead(II) halides in toluene or dichloromethane affords the adducts $[Cl_2M\{(\mu_3\text{-}NH)_3Ti_3(\eta^5\text{-}C_5Me_5)_3(\mu_3\text{-}N)\}]$ (M = Sn (**10**), Pb(**11**)) or $[I_2Sn\{(\mu_3\text{-}NH)_3Ti_3(\eta^5\text{-}C_5Me_5)_3(\mu_3\text{-}N)\}]$ (**12**) as orange or brown solvent-free solids in 60–81 % yields. Alternatively, crystals of **12** were obtained upon heating a mixture of **10** with methyl iodide in [D_6]benzene at 60 °C for six days.

Attempts to prepare other metal dihalide adducts failed. For instance, $CaCl_2$ did not react with **1** under the same conditions, and $[GeCl_2(dioxane)_2]$ gave complicated mixtures of products.

Alkaline-earth metal adducts **7**–**9** were characterized by spectral and analytical techniques. IR spectra (KBr) reveal two ν_{NH} vibrations in the range 3337–3236 cm^{-1}. ^{1}H and

$^{13}C\{^1H\}$ NMR spectra in [D_1]chloroform at room temperature are consistent with the tridentate coordination of **1** to the alkaline-earth metal centers. Their ^1H NMR spectra show single resonances for the NH and η^5-C_5Me_5 groups, suggesting the existence of a dynamic behavior in solution. We have reported analogous spectroscopic data for the ionic azaheterometallocubane complexes [{(cod)M(μ_3-NH)$_3$Ti$_3$(η^5-C_5Me_5)$_3$(μ_3-N)}(X)] (M = Rh, Ir; X = Cl, BPh_4; cod = 1,5-cyclooctadiene),[6] which present a trigonal-bypiramidal geometry around the Group 9 metal centers.

Again the attempts to obtain single crystals for X-ray crystallographic studies of complexes **7–9** were unsuccessful; therefore DFT calculations were carried out to study the structures for model compounds. The most stable geometry in the CaI_2 complex for a five-coordinate environment corresponds to a distorted tetragonal pyramid, although the trigonal-bypiramid structure is only 2 kJ mol^{-1} above (Scheme 5).

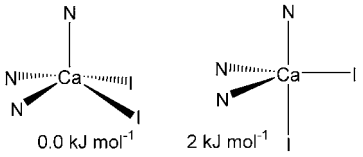

Scheme 5. Calculated geometries and relative energy values for the [I_2Ca{(μ_3-NH)$_3$Ti$_3$(η^5-C_5H_5)$_3$(μ_3-N)}] complex.

Only monomer structures have been considered in the DFT studies, although it is also reasonable that dimeric or even oligomeric species, generated through iodide bridging atoms, might be favored in the solid state. The lack of volatility of these complexes precluded the possibility to gain information by mass spectrometry. Furthermore, complexes **7–9** are not soluble in aromatic solvents and exhibit a low solubility in chloroform or dichloromethane, suggesting a higher aggregation state in the solid state.

Group 14 complexes **10–12** were characterized by spectral and analytical techniques, as well as by X-ray crystal structure determinations for **10** and **12**. IR spectra (KBr) reveal ν_{NH} vibrations in the range 3343–3286 cm^{-1}. ^1H and $^{13}C\{^1H\}$ NMR spectra for **10–12** in [D_1]chloroform at room temperature reveal the equivalence of the NH and η^5-C_5Me_5 groups.

The molecular structure of **10** is presented in Figure 2 and selected distances and angles are given in Table 1.[17] Two independent molecules of **10** are found in the asymmetric unit, which may be weakly associated by a Sn1···Sn2 (4.446(2) Å) interaction, the length of which is slightly shorter than the sum of the van der Waals radii (4.52 Å) and similar to other Sn···Sn distances found in the literature.[18,19] If this Sn···Sn interaction is taken into account, the geometry for the tin atoms can be defined as pseudo-tetrahedral, although a trigonal-prism environment can be visualized if all the imido-nitrogen atoms are considered.

Within the same molecule, the tin atom is coordinated to two chlorine and one imido-nitrogen atoms. The Sn–Cl[18] (2.541(1) Å) and Sn1–N23 (2.285(3) Å) or Sn2–N46 (2.264(4) Å)[18a,20] bond lengths are similar to others found for tin(II) compounds. Furthermore, these Sn–N bonds are approximately 0.8 Å shorter than the other two Sn–N distances of each molecule, suggesting the absence of any important interaction between the rest of the imido groups and the tin atoms (see Table 1). However, the ^1H NMR spectrum of **10** in [D_2]dichloromethane, even at −80 °C, shows single sharp resonances for the NH and η^5-C_5Me_5 ligands, suggesting the existence of a dynamic process with a low-energy barrier.

The incorporation of the tin atom to the preorganized ligand does not affect significantly to the average bond distances and angles within the organometallic fragment, presenting values close to those found for the parental compound **1**.[1]

The molecular structure of complex **12** is presented in Figure 3 and selected distances and angles are given in

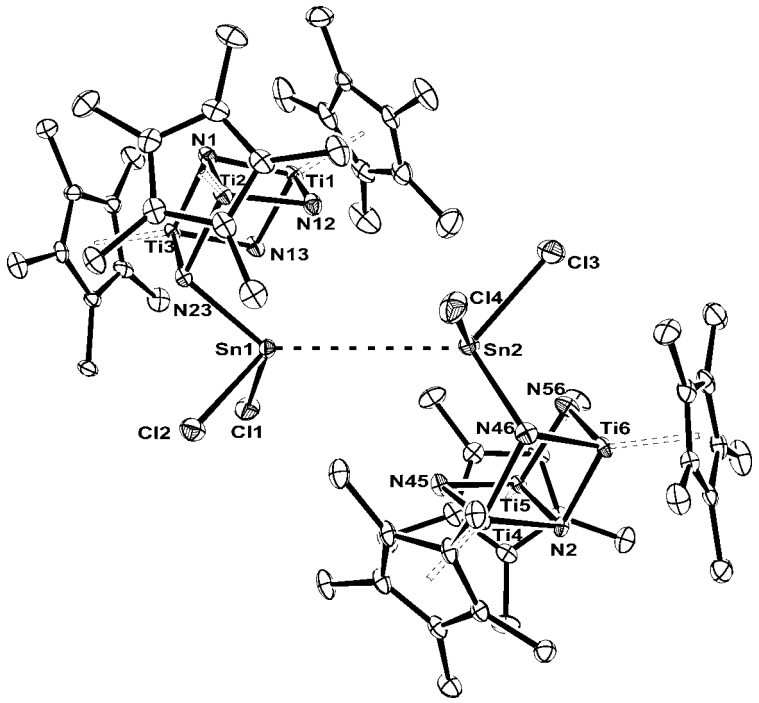

Figure 2. Molecular structure of **10**.

Table 1. Average and selected lengths [Å] and angles [°] for **10**.

Molecule 1		Molecule 2	
Ti···Ti	2.833(1)	Ti···Ti	2.838(1)
N1–Ti	1.928(3)	N2–Ti	1.930(3)
N12–Ti2	1.903(4)	N45–Ti4	1.903(3)
N12–Ti1	1.957(4)	N45–Ti5	1.956(3)
N13–Ti3	1.919(4)	N46–Ti6	1.999(4)
N13–Ti1	1.950(4)	N46–Ti4	2.022(4)
N23–Ti3	1.991(4)	N56–Ti6	1.917(4)
N23–Ti2	2.021(3)	N56–Ti5	1.965(4)
N23–Sn1	2.285(3)	N46–Sn2	2.264(4)
Cl1–Sn1	2.520(1)	Cl3–Sn2	2.522(1)
Cl2–Sn1	2.567(1)	Cl4–Sn2	2.556(1)
Sn1···N12	3.163(4)	Sn2···N45	3.196(4)
Sn1···N13	3.030(5)	Sn2···N56	3.038(4)
Sn1···Ti1	3.858(1)	Sn2···Ti4	3.480(2)
Sn1···Ti2	3.466(1)	Sn2···Ti5	3.883(2)
Sn1···Ti3	3.428(1)	Sn2···Ti6	3.398(2)
Sn1···Sn2	4.446(2)		
N23-Sn1-Cl1	110.5(1)	N46-Sn2-Cl3	107.4(1)
N23-Sn1-Cl2	83.1(1)	N46-Sn2-Cl4	83.1(1)
Cl1-Sn1-Cl2	90.6(1)	Cl3-Sn2-Cl4	89.6(1)
Ti-N1-Ti	94.5(1)	Ti-N2-Ti	94.7(1)
Ti1-N12-Ti2	93.9(2)	Ti4-N45-Ti5	94.1(1)
Ti1-N13-Ti3	93.8(2)	Ti4-N46-Ti6	90.9(1)
Ti2-N23-Ti3	90.6(1)	Ti5-N56-Ti6	93.4(2)
N1-Ti-N	86.2(2)	N2-Ti-N	86.1(2)
N12-Ti1-N13	105.2(2)	N45-Ti4-N46	100.8(2)
N12-Ti2-N23	100.9(2)	N45-Ti5-N56	105.3(2)
N13-Ti3-N23	98.2(2)	N46-Ti6-N56	99.0(2)

Table 2. Average and selected lengths [Å] and angles [°] for **12**.

Sn1···Ti	3.288(1)	Ti···Ti	2.834(1)
Sn1···Sn1	4.688(1)	Ti-N1	1.921(3)
Sn1–I1	3.494(1)	Ti1–N11	1.963(3)
Sn1–I2	3.300(1)	Ti1–N12	1.958(3)
Sn1–N11	2.427(4)	Ti2–N12	1.965(3)
Sn1–N12	2.545(3)	N11···I2	3.522(1)
		I2···H11	2.897
Sn1-I1-Sn1	84.3(1)	Ti-N1-Ti	95.1(1)
I1-Sn1-I1	95.7(1)	Ti1-N11-Ti1	93.0(2)
I1-Sn1-I2	101.2(1)	Ti1-N11-Sn1	95.5(1)
I1-Sn1-N11	132.1(1)	Ti1-N12-Ti2	92.2(1)
I1-Sn1-N12	128.4(1)	Ti1-N12-Sn1	92.0(1)
I2-Sn1-N11	74.1(1)	Ti2-N12-Sn1	94.5(1)
I2-Sn1-N12	130.4(1)	N1-Ti-N	86.2(2)
N11-H11···I2	129	N-Ti-N	98.1(2)

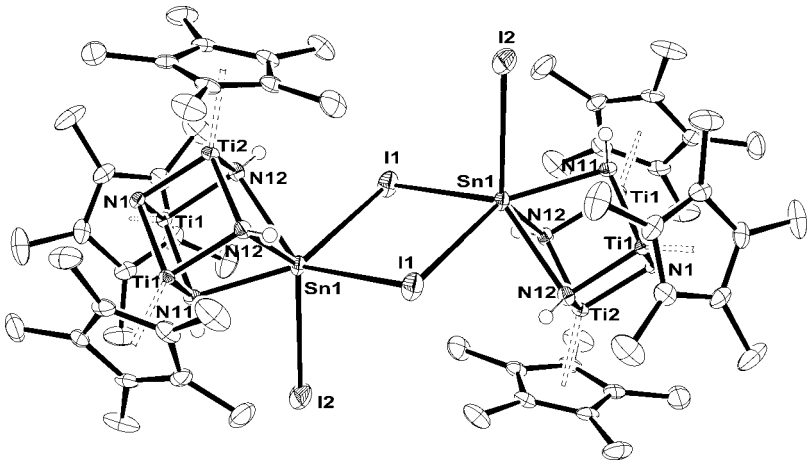

Figure 3. Molecular structure of **12**.

Table 2.[17] The structure contains two $SnTi_3N_4$ cube units linked by two bridging iodine atoms and related by a center of symmetry located in the middle of the planar Sn_2I_2 moiety. The molecule also presents a mirror plane which contains the Sn1, Ti2, N1, N11, H11, and I2 atoms from the core. The distance between the two tin atoms is 4.688(1) Å, and thus longer than the sum of the van der Waals radii.

The Sn–I bond lengths [(bridging 3.494(1), and terminal 3.300(1) Å) are similar to the values found in other compounds containing polimeric μ-I bridged Sn_2I_2 units.[21]

The structural disposition of the ligands around the tin atoms is trigonal prismatic; the iodine atoms are situated in an eclipsed conformation with respect to the imido-nitrogen atoms. The distances I2···N11 (3.522(1) Å) and I2···H11 (2.897 Å), which are located in the mirror plane of the molecule, might be indicative of hydrogen bonding.[17,22]

Similarly to **10**, within the organometallic ligand of **12** the structural parameters do not differ significantly with respect to the free complex **1**, except for the value of the N_{imido}-Ti-N_{imido} angle that is approximately 9° narrower in the case of **12**. This variation may be directly attributed to the coordination of the three imido groups to the metal center; the Sn–N distances of 2.427(4) and 2.545(3) Å are ≈0.2 Å longer than those in **10**, and are in agreement with the increase in the coordination number from four, in the analogous chloride complex, to six.

DFT calculations were carried out for monomeric tin and lead model compounds. For the $SnCl_2$ complex, these calculations reproduce well the Sn–Cl distances, internal core angles, and the existence of one short and two long Sn–N distances, being respectively 0.1 and 0.2 Å longer than the experimental values.

The most stable environment for the incorporated metal atom is in all the cases pseudo-octahedral, with one of the positions being occupied by the lone pair. But the trigonal-prismatic disposition, in which the metal lone pair and the halogens are eclipsed with respect to the three NH ligands, is only 7–10 kJ mol^{-1} higher in energy (in the case of metal chlorides).

Coordination of [{Ti(η^5-C_5Me_5)(μ-NH)}$_3$(μ$_3$-N)] to metal trihalides MX_3: Addition of indium triiodide to one equivalent

of **1** in toluene at room temperature affords $[I_3In\{(\mu_3\text{-}NH)_3Ti_3(\eta^5\text{-}C_5Me_5)_3(\mu_3\text{-}N)\}]$ (**13**, 80%) as brown crystals (Scheme 6). Analogous reactions with indium trichloride or aluminum tribromide gave intractable mixtures of products, presumably by activation of N–H bonds and generation of reactive HX.

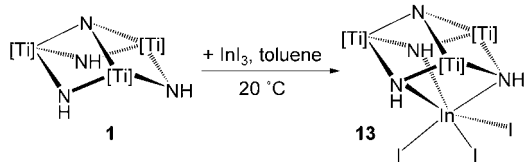

Scheme 6. Synthesis of complex **13**. $[Ti] = Ti(\eta^5\text{-}C_5Me_5)$.

Table 3. Selected bond lengths [Å] and angles [°] for **13**.

In1–I1	2.764(3)	Ti···Ti	2.820(4)
In1–I2	2.740(2)	Ti–N1	1.914(14)
In1–I3	2.700(2)	Ti1–N12	2.023(16)
In1–N12	2.199(16)	Ti1–N13	1.892(15)
In1···N13	3.261(19)	Ti2–N12	2.044(17)
In1···N23	3.501(19)	Ti2–N23	1.874(15)
		Ti3–N13	1.946(17)
		Ti3–N23	1.919(16)
I-In1-I	104.6(9)	Ti-N1-Ti	94.9(6)
I1-In1-N12	94.0(4)	N1-Ti-N	86.06)
I2-In1-N12	122.7(4)	Ti1-N12-Ti2	89.2(7)
I3-In1-N12	123.1(4)	Ti1-N13-Ti3	94.0(7)
Ti1-N12-In1	109.4(7)	Ti2-N23-Ti3	95.0(7)
Ti2-N12-In1	115.7(7)	N12-Ti1-N13	99.6(7)
		N12-Ti2-N23	101.9(7)
		N13-Ti3-N23	107.3(7)

Complex **13** was characterized by spectral and analytical techniques, as well as by an X-ray crystal structure determination. Mass spectrometry (EI, 70 EV) supports a monomer formulation in the gas phase for **13**. IR spectra (KBr) revealed two ν_{NH} vibrations for the NH groups in the molecule at 3358 and 3279 cm^{-1}. ^1H and $^{13}C\{^1H\}$ NMR spectra in $[D_1]$chloroform at room temperature show equivalent NH and $\eta^5\text{-}C_5Me_5$ groups in solution.

The molecular structure of **13** is presented in Figure 4 and selected distances and angles are given in Table 3.[17] The solid-state structure reveals a distorted tetrahedral geometry for the indium center, comprising three iodide and one NH group with angles spanning 94.0(4)–123.1(4)°. But if all the imido-nitrogen atoms are considered, the environment around the indium atom is best visualized as trigonal-prismatic, in a fashion similar to the structure of **10**. The In–I bond lengths range from 2.700(2) to 2.764(3) Å and compare well with those reported for other $[InI_3(L)_x]$ ($x = 1$, 2, 3) complexes.[23]

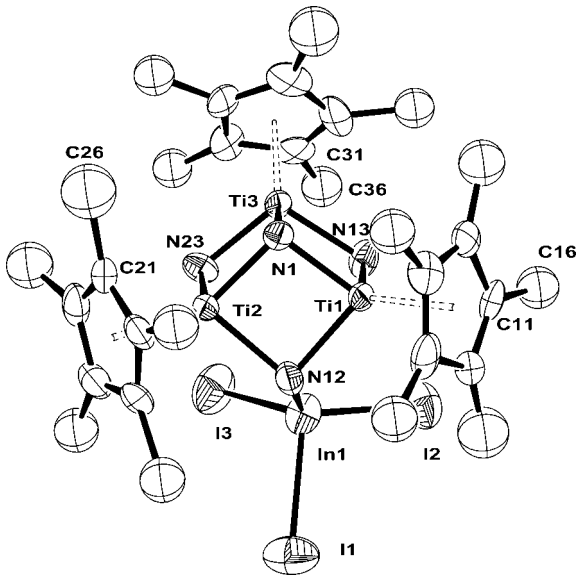

Figure 4. Molecular structure of **13**.

The In–N12 bond length of 2.199(16) Å is slightly short for a dative bond.[23,24] This In–N distance is in the same range to those found for amido-, imido-, and tris(pyrazolyl)-boratoindium(III) derivatives.[25] The remaining NH groups from the triaza ligand are clearly not coordinated to the indium center (distances In1···N13 3.261(19) Å; In1···N23 3.499 Å) in contrast to the situation determined for the triazacyclononane $[InBr_3(Me_3[9]aneN_3)]$,[26] the triazacyclohexane $[InBr_3\{\text{-}N(Me)\text{-}CH_2\text{-}\}_3]$,[26] and $[InMe_3\{\text{-}N(i\text{Pr})\text{-}CH_2\text{-}\}_3]$ complexes.[27]

In a similar way to that in complex **10**, the average bond lengths and angles within the organometallic fragment in **13** are similar to those found for the free ligand **1**.[1]

DFT calculations on compound **13** reproduce the X-ray crystal structure in which the metal is linked to the tripodal ligand by a dative M–NH bond. The computed In–N bond length of 2.252 Å is 0.05 Å longer than the experimentally determined distance. The deviation is notably larger for the nonbonded interactions between the indium and the other two NH groups (~0.4 Å). However, the geometry for which the two nonbonded In–N distances are fixed at the average experimental value of 3.38 Å is only 10.9 $kJ\,mol^{-1}$ above the fully optimized geometry. This small energy difference indicates that the potential surface is very flat, and suggests that the differences between the calculated and experimental geometrical parameters could be due to intermolecular interactions in the solid phase. When the C_{3v} symmetry is imposed, all the three In–NH distances are equal to 2.658 Å, and the resulting structure is about 30 $kJ\,mol^{-1}$ higher in energy than the asymmetric one. This relatively small energy is in agreement with the ^1H NMR spectrum in $[D_2]$dichloromethane at −80 °C of **13**, which shows only a single sharp resonance for the C_5Me_5 ligands.

After reviewing all the results, it seems that a trigonal-prismatic conformation for the MX_n adducts is preferred. In this disposition the halide atoms can occupy a less crowded space and thus minimize the steric interaction with the pen-

tamethylcyclopentadienyl groups linked to the titanium atoms.

Reaction energies for the formation of the [1−MXn] adducts: A series of DFT calculations were carried out to understand the adduct formation reactions between metal halides MX_n and the organometallic ligand **1.**

Calculated reaction energies for alkali-metal halides MX with **1** are given in Figure 5. In the gas phase, that is, when the solvent is not considered, the formation of [**1**–MX] from

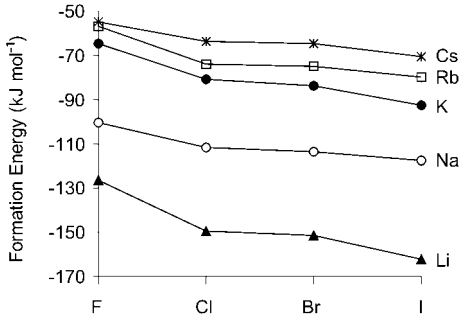

Figure 5. Calculated reaction energies for **1** and alkali-metal halides MX in the gas phase.

1 and MX is computed to be a largely exothermic process (from −55 to −162 kJ mol^{-1}). These values increase going down the halogen group and going up the alkali-metal group. For the Tl and In monohalides the processes are also exothermic with lower reactions energies (from −50 to −70 kJ mol^{-1}). Results of DFT calculations are consistent with the trends observed for the obtained [**1**–MX] complexes, but they cannot completely explain all the experimental results (see below).

Binding energies indicate that there is a strong relationship between the reaction energy and the nature of the MX bond. Electron density difference (EDD) maps were computed as the difference between the electron density of the [**1**–MX] complex and the electron density of the fragments MX and **1** at the geometry of the optimized complex. Figure 6 contains EDD maps for the LiCl, LiI, NaI, and KI halide complexes. These maps clearly show that the formation of the M−N bonds is accompanied by an important electron density accumulation in the interacting region between the two fragments. Bonding energies and the charge density accumulations are related; thus, the largest electronic reorganization occurs for lithium iodide (Figure 6b), that is the complex with the largest bonding energy between **1** and the halide. When the halogen is chlorine the bonding energy and the electronic reorganization are slightly smaller (Figure 6a). The electronic changes are significantly smaller when the metal is sodium (Figure 6c). It is well-known that Li^+ is a highly polarizing ion and that it can induce a strong polarization in the tripodal ligand. Consequently the largest interaction energies appear for the lithium series.

When going down the halogen group the LUMO of MX, which is an almost pure *n*s and *n*p metal orbital, drops in energy favoring the mixing with the lone pair orbitals of the tridentate ligand. Hence, for example, for LiF the energy of the LUMO (with a composition of 73% $2s_{Li}$ and 17% $2p_{Li}$) is −1.40 eV, whereas for LiCl the corresponding energy is −1.93 eV (83% $2s_{Li}$ and 13% $2p_{Li}$). But this dependence of the bonding energy on the halogen is minor compared to that found with respect to the metal, which is the dominant factor as Figure 5 clearly shows.

Reaction energies for a series of [**1**–MX_2] (M = alkaline-earth metal) complexes were also computed (see Supporting Information). In general, these processes are quite exothermic (ranging from −128 to −241 kJ mol^{-1}) and higher than those calculated for the Group 1 adducts; the calcium derivatives display the largest values. As for the alkali-metal complexes, the greatest formation energy in each series was found for the iodide derivatives. Calculations were also carried out for tin and lead halide complexes. In the lead series,

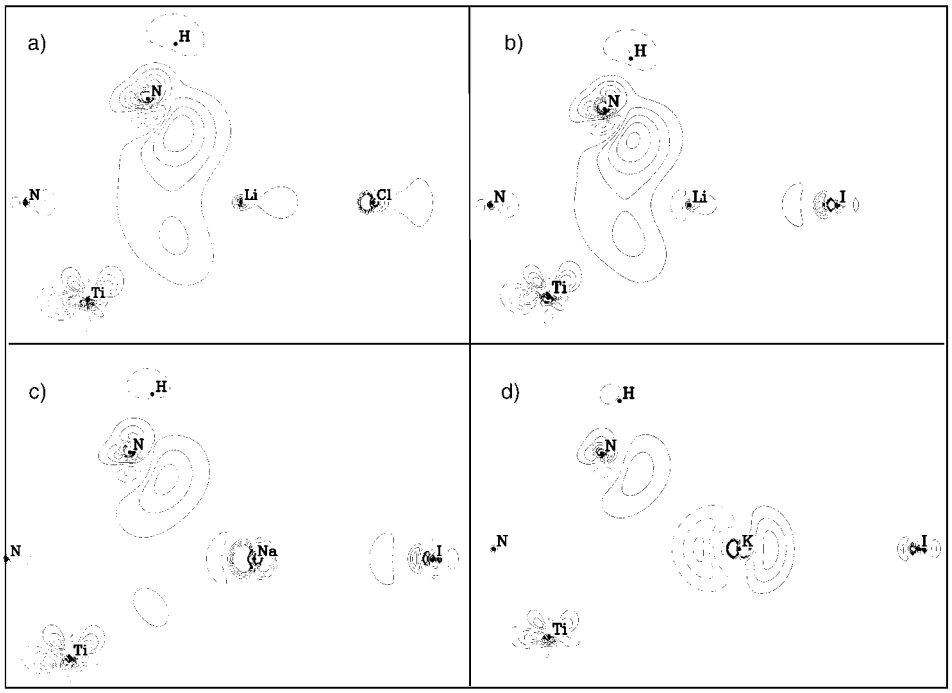

Figure 6. Electron density difference maps of a) LiCl, b) LiI, c) NaI, and d) KI halide complexes. The density difference is shown in a σ_v symmetry plane. Positive contours indicate electron density accumulation.

the differences in the reaction energies are quite small (~6 kJ mol^{-1}). For the [**1**−MX_3] (M = In, Tl; X = F, I) complexes the reaction energies range between −85 and −160 kJ mol^{-1}. Interestingly, in these complexes the coordination energy of the MX_3 group to the tripodal ligand is smaller when the halogen is iodine.

Solvent effects: Although the reactions between **1** and the MX_n salts were computed to be highly exothermic as indicated above, **1** does not react with some of the metal halides. How should we interpret this experimental behavior? Lattice energies of the MX_n salts seem to play a crucial role in these processes. The reactions have been carried out with the halides in the solid state and therefore the dissolution of the metal halides must also be taken into account in the energetic balance. The reaction energy, ΔE, for the process **1**(soln) + MX(s)→[**1**–MX](soln) is the sum of two energies: dissolution of MX(s)(ΔE_1) and formation of [**1**–MX] in solution (ΔE_2).

Because ΔE_1 is always positive, the formation of the [**1**–MX] complex will require that ΔE_2 overcomes the dissolution energy of the solid salt, or at least that the global process should not be largely endothermic. In solution, the reaction energy ΔE_2 depends on the nature of the solvent. At present, it is still not possible to take into account in a quantum-chemistry study all factors that have an influence on chemical reactions in solution. However, a first-order approximation for dilute solutions is to model the solvent effects by a polarizable continuum.[28] The [**1**–MX] formation energies (ΔE_2) in toluene or dichloromethane were computed for several lithium halides (Table 4).

Table 4. Computed and estimated energies [kJ mol^{-1}] for several steps in the formation of [**1**-LiX] in toluene and dichloromethane.

Step	Energy	Method	Halogen			
			F	Cl	Br	I
				toluene		
1(soln) + LiX(soln)→**1**-LiX(soln)	ΔE_2	DFT+COSMO	−94.0	−92.1	−107.4	−117.8
LiX(g)→LiX(soln)	ΔE_3	DFT+COSMO	−74.7	−73.1	−66.6	−63.6
LiX(s)→LiX(soln)	ΔE_1	expt[a]	204.5	139.6	130.3	115.3
1(soln) + LiX(s)→**1**-LiX(soln)	ΔE	$\Delta E_1+\Delta E_2$	110.5	47.5	22.9	−2.5
				dichloromethane		
1(soln) + LiX(soln)→**1**-LiX(soln)	ΔE_2	DFT+COSMO	−69.9	−77.7	−73.8	−83.7
LiX(g)→LiX(soln)	ΔE_3	DFT+COSMO	−126.0	−130.5	−122.2	−119.0
LiX(s)→LiX(soln)	ΔE_1	expt[a]	153.0	82.3	74.6	59.7
1(soln) + LiX(s)→**1**-LiX(soln)	ΔE	$\Delta E_1+\Delta E_2$	83.1	4.6	0.8	−24.0

[a] The dissolution energies of the solid (ΔE_1) are estimated from the experimental energies of condensation (LiX(g)→LiX(s) taken from reference[29]) and from the computed energy of dissolution of the gas(ΔE_3).

Although the reaction energies have the same trends found for the gas phase (Figure 5), they are significantly smaller. Values for ΔE_2 suggest that polar solvents do not favor directly the complexation of **1** and MX in solution because the MX dipole is strongly stabilized in polar solvents. In the overall balance of the reaction energy, ΔE_1 is also very important. This energy has been estimated from the experimental energies of condensation[29,30] and the solvation energies computed for MX.

The dissolution energy of LiX in toluene decreases on going down the halogen group (Table 4), therefore LiI is the salt easier to dissolve. Because the largest reaction energy, ΔE_2, also occurs for LiI, the formation of [**1**–LiI] is the most favorable. The process in this case is slightly exothermic in toluene ($\Delta E = -2.5$ kJ mol^{-1}). In dichloromethane all values of ΔE are shifted towards more negative values. Thus, despite the fact that the reactions are less exothermic, the formation of this kind of complexes is easier in polar solvents.

The ΔE value was also computed for the TlI and InI derivatives (see Supporting Information), complexes with relatively small binding energies in the gas phase (−65.1 and −71.0 kJ mol^{-1}, respectively). However, both complexes have been experimentally obtained. As for the lithium derivatives, the incorporation of solvent in the calculations reduces the values of the reaction energies (−17.2, −19.9 kJ mol^{-1}). The dissolution energies of TlI(s) and InI(s) are only slightly higher than the reaction energies, therefore the global processes are slightly endothermic (+13.8 and +2.3 kJ mol^{-1} for InI and TlI, respectively).

Conclusions and Perspectives

The reactions described herein demonstrate the ability of the imido-nitrido complex [{Ti(η^5-C_5Me_5)(μ-NH)}$_3$(μ_3-N)] (**1**) to produce the rupture of highly stable metal halide lattices to yield molecular complexes. DFT calculations show that the reactions are energetically favorable in the gas phase, but the lattice energies of the MX_n salts and the nature of the solvent used must be taken into account to determine the viability of the processes. Furthermore, in the solid state and/or solution, complex **1** shows a flexible behavior both as a monodentate or a tridentate ligand towards the main group metal halides.

In the future we hope to expand this study with other inorganic combinations with the aim to uncover more novel findings in the area of metal nitrido complexes.

Experimental Section

General considerations: All manipulations were carried out under an argon atmosphere using Schlenk line or glovebox techniques. Hexane was distilled from Na/K alloy just prior to use. Toluene was freshly distilled from sodium. Dichloromethane was distilled from P_2O_5. NMR solvents were dried with CaH_2 ($CDCl_3$) or Na/K alloy (C_6D_6) and vacuum-distilled. Oven-dried glassware was repeatedly evacuated with a pumping

system (ca. 1×10^{-3} Torr) and subsequently filled with inert gas. Metal halides MX_n were purchased from Aldrich, ground up, and heated under vacuum prior to use. [{Ti(η^5-C_5Me_5)(μ-NH)}$_3$(μ_3-N)] (**1**),[2] and [{Li[(μ_3-NH)$_2$(μ_3-N){Ti$_3$(η^5-C_5Me_5)$_3$(μ_3-N)}]}$_2$][5] were prepared according to published procedures.

Samples for infrared spectroscopy were prepared as KBr pellets. ^{1}H and ^{13}C{^{1}H} NMR spectra were recorded on a Varian Unity-300 spectrometer. Chemical shifts (δ) are given relative to residual protons or to carbon of the solvent. Electron impact mass spectra were obtained at 70 eV. Microanalysis (C, H, N) were performed on a Leco CHNS-932 microanalyzer, except those for the complex [{ISn(μ_3-NH)$_3$Ti$_3$(η^5-C_5Me_5)$_3$(μ_3-N)}$_2$(μ-I)$_2$]·C_6D_6 which were performed on a Perkin Elmer PE 2400 Serie II CHNS/O microanalyzer.

Synthesis of [BrLi{(μ_3-NH)$_3$Ti$_3$(η^5-C_5Me_5)$_3$(μ_3-N)}] (2): A 100-mL Schlenk flask was charged with **1** (0.30 g, 0.49 mmol), LiBr (0.043 g, 0.49 mmol), and toluene (40 mL). The reaction mixture was stirred at room temperature for 20 h. The resultant brown solution was filtered and the volatile components were removed under reduced pressure to give a brown solid. The solid was washed with hexane (20 mL) and then dried under vacuum to yield **2** as a yellow powder (0.23 g, 67%). IR (KBr): $\tilde{\nu}$= 3349 (m), 2909 (s), 2858 (s), 1490 (m), 1429 (m), 1377 (m), 1261 (w), 1066 (w), 1026 (m), 711 (s), 663 (vs), 643 (s), 627 (m), 574 (m), 480 (w), 432 cm^{-1} (m); ^{1}H NMR (300 MHz, C_6D_6, 20°C, TMS): δ=12.88 (s br., 3H; NH), 1.98 ppm (s, 45H; C_5Me_5); ^{13}C{^{1}H} NMR (75 MHz, C_6D_6, 20°C, TMS): δ=119.3 (C_5Me_5), 11.8 ppm (C_5Me_5); MS (EI, 70 eV): *m*/*z* (%): 695 (1) [*M*]$^+$, 559 (11) [*M*−C_5Me_5H]$^+$, 423 (8) [*M*−2C_5Me_5H]$^+$, 287 (7) [*M*−3C_5Me_5H]$^+$; elemental analysis calcd (%) for $C_{30}H_{48}BrLiN_4Ti_3$: C 51.83, H 6.96, N 8.06; found: C 52.16, H 7.08, N 7.34.

Synthesis of [ILi{(μ_3-NH)$_3$Ti$_3$(η^5-C_5Me_5)$_3$(μ_3-N)}] (3): In a similar fashion to the preparation of **2**, **1** (0.30 g, 0.49 mmol) and LiI (0.066 g, 0.49 mmol) were allowed to react in toluene (40 mL) for five days to afford **3** as a pale yellow solid (0.29 g, 65%). IR (KBr): $\tilde{\nu}$=3346 (m), 2909 (s), 2858 (s), 1490 (m), 1429 (m), 1377 (s), 1260 (w), 1067 (w), 1026 (m), 790 (vs), 709 (s), 659 (vs), 626 (m), 584 (m), 480 (w), 433 cm^{-1} (m); ^{1}H NMR (300 MHz, C_6D_6, 20°C, TMS): δ=12.77 (s br., 3H; NH), 1.88 ppm (s, 45H; C_5Me_5); ^{13}C{^{1}H} NMR (75 MHz, C_6D_6, 20°C, TMS): δ=120.0 (C_5Me_5), 11.9 ppm (C_5Me_5); elemental analysis calcd (%) for $C_{30}H_{48}ILiN_4Ti_3$: C 48.55, H 6.52, N 7.55; found: C 48.42, H 6.08, N 6.13.

Synthesis of [INa{(μ_3-NH)$_3$Ti$_3$(η^5-C_5Me_5)$_3$(μ_3-N)}] (4): In a fashion similar to the preparation of **2**, **1** (0.30 g, 0.49 mmol) and NaI (0.074 g, 0.49 mmol) were allowed to react in toluene (40 mL) for two days to afford **4** as a yellow solid (0.18 g, 48%). IR (KBr): $\tilde{\nu}$=3337 (m), 2908 (s), 2857 (s), 1490 (m), 1429 (m), 1376 (s), 1261 (w), 1066 (w), 1026 (m), 787 (m), 748 (s), 712 (s), 679 (vs), 659 (vs), 643 (s), 626 (m), 579 (m), 476 (m), 429 cm^{-1} (m); ^{1}H NMR (300 MHz, C_6D_6, 20°C, TMS): δ=13.22 (s br., 3H; NH), 2.03 ppm (s, 45H; C_5Me_5); ^{13}C{^{1}H} NMR (75 MHz, C_6D_6, 20°C, TMS): δ=118.9 (C_5Me_5), 12.2 ppm (C_5Me_5); MS (EI, 70 eV): *m*/*z* (%): 758 (1) [*M*]$^+$, 486 (1) [*M*−2C_5Me_5H]$^+$; elemental analysis calcd (%) for $C_{30}H_{48}IN_4NaTi_3$: C 47.52, H 6.38, N 7.39; found: C 47.56, H 6.38, N 6.59.

Synthesis of [IIn{(μ_3-NH)$_3$Ti$_3$(η^5-C_5Me_5)$_3$(μ_3-N)}] (5): In a fashion similar to the preparation of **2**, **1** (0.30 g, 0.49 mmol) and InI (0.119 g, 0.49 mmol) were allowed to react in dichloromethane (150 mL) for three days. After filtration, the volatile components were removed under reduced pressure, and the resultant solid washed with toluene (20 mL) and dried under vacuum to afford **5** as a brown powder (0.29 g, 69%). IR (KBr): $\tilde{\nu}$=3350 (w), 3246 (m), 2908 (s), 2856 (m), 1489 (w), 1427 (m), 1377 (m), 1261 (w), 1066 (w), 1025 (m), 776 (m), 711(s), 659 (vs), 529 (m), 476 (m), 429 cm^{-1} (m); ^{1}H NMR (300 MHz, C_6D_6, 20°C, TMS): δ= 12.87 (s br., 3H; NH), 2.01 ppm (s, 45H; C_5Me_5); ^{13}C{^{1}H} NMR (75 MHz, C_6D_6, 20°C, TMS): δ=117.9 (C_5Me_5), 11.9 ppm (C_5Me_5); elemental analysis calcd (%) for $C_{30}H_{48}IInN_4Ti_3$: C 42.39, H 5.69, N 6.59; found: C 42.32, H 5.57, N 6.27.

Synthesis of [ITl{(μ_3-NH)$_3$Ti$_3$(η^5-C_5Me_5)$_3$(μ_3-N)}] (6): In a fashion similar to the preparation of **5**, **1** (0.30 g, 0.49 mmol) and TlI (0.163 g, 0.49 mmol) were allowed to react in dichloromethane (50 mL) for seven days to afford **6** as a yellow powder (0.32 g, 70%). IR (KBr): $\tilde{\nu}$=3352 (w), 3301 (m), 2907 (s), 2856 (m), 1489 (w), 1449 (m), 1429 (m), 1377 (m), 1257 (w), 1155 (w), 1066 (w), 1025 (w), 761 (m), 719 (m), 667 (vs), 642 (s), 528 (w), 476 (w), 427 cm^{-1} (m); ^{1}H NMR (300 MHz, C_6D_6, 20°C, TMS): δ=13.57 (s br., 3H; NH), 2.02 ppm (s, 45H; C_5Me_5); ^{13}C{^{1}H} NMR (75 MHz, C_6D_6, 20°C, TMS): δ=118.8 (C_5Me_5), 12.0 ppm (C_5Me_5); elemental analysis calcd (%) for $C_{30}H_{48}IN_4Ti_3Tl$: C 38.35, H 5.15, N 5.96; found: C 38.40, H 5.32, N 5.69.

Reaction of 1 with LiCl generated in situ: A 100-mL Schlenk flask was charged with [Li{(μ_3-NH)$_2$(μ_4-N){Ti$_3$(η^5-C_5Me_5)$_3$(μ_3-N)}]$_2$ (0.19, 0.14 mmol), NEt_3HCl (0.039 g, 0.28 mmol), and toluene (25 mL). The reaction mixture was stirred for 14 h at room temperature to give an orange solution with a white fine powder in suspension. After filtration, the solution was dried to give an orange solid identified as **1** by NMR spectroscopy.[2]

Synthesis of [I$_2$Mg{(μ_3-NH)$_3$Ti$_3$(η^5-C_5Me_5)$_3$(μ_3-N)}] (7): In a fashion similar to the preparation of **5**, **1** (0.30 g, 0.49 mmol) and MgI_2 (0.137 g, 0.49 mmol) were allowed to react in dichloromethane (40 mL) for 24 h to afford **7** as a yellow powder (0.24 g, 55%). IR (KBr): $\tilde{\nu}$=3337 (s), 3236 (w), 2945 (m), 2910 (s), 2858 (m), 1489 (m), 1427 (m), 1379 (s), 1205 (w), 1067 (w), 1025 (m), 778 (s), 736 (s), 700 (s), 665 (vs), 535 (w), 480 (m), 438 cm^{-1} (m); ^{1}H NMR (300 MHz, $CDCl_3$, 20°C, TMS): δ=11.80 (s br., 3H; NH), 2.14 ppm (s, 45H; C_5Me_5); ^{13}C{^{1}H} NMR (75 MHz, $CDCl_3$, 20°C, TMS): δ=123.2 (C_5Me_5), 12.7 ppm (C_5Me_5); elemental analysis calcd (%) for $C_{30}H_{48}I_2MgN_4Ti_3$: C 40.65, H 5.46, N 6.32; found: C 40.82, H 5.66, N 5.88.

Synthesis of [I$_2$Ca{(μ_3-NH)$_3$Ti$_3$(η^5-C_5Me_5)$_3$(μ_3-N)}] (8): In a fashion similar to the preparation of **5**, **1** (0.50 g, 0.82 mmol) and CaI_2 (0.201 g, 0.68 mmol) were allowed to react in dichloromethane (100 mL) for four days to afford **8** as a pale yellow solid (0.43 g, 69%). IR (KBr): $\tilde{\nu}$=3327 (m), 3306 (m), 2910 (s), 2858 (m), 1494 (m), 1428 (m), 1379 (s), 1068 (w), 1027 (m), 788 (m), 746 (s), 733 (s), 674 (vs), 664 (vs), 659 (vs), 648 (vs), 535 (w), 479 (m), 435 cm^{-1} (m); ^{1}H NMR (300 MHz, $CDCl_3$, 20°C, TMS): δ=13.08 (s br., 3H; NH), 2.12 ppm (s, 45H; C_5Me_5); ^{13}C{^{1}H} NMR (75 MHz, $CDCl_3$, 20°C, TMS): δ=121.8 (C_5Me_5), 12.5 ppm (C_5Me_5); elemental analysis calcd (%) for $C_{30}H_{48}CaI_2N_4Ti_3$: C 39.94, H 5.36, N 6.21; found: C 40.04, H 5.49, N 4.97.

Synthesis of [I$_2$Sr{(μ_3-NH)$_3$Ti$_3$(η^5-C_5Me_5)$_3$(μ_3-N)}] (9): In a 100-mL Schlenk flask, **1** (0.30 g, 0.49 mmol) and SrI_2 (0.15 g, 0.44 mmol) were allowed to react at room temperature in dichloromethane (25 mL) for six days to afford a yellow precipitate and a brown solution. The solution was removed by filtration and the precipitate washed with toluene (15 mL) and vacuum-dried to give **9** as a pale yellow powder (0.37 g, 89%). IR (KBr): $\tilde{\nu}$=3325 (m), 3310 (m), 2911 (s), 2858 (m), 1489 (m), 1428 (m), 1379 (s), 1263 (m), 1067 (w), 1026 (m), 785 (m), 744 (s), 670 (vs), 655 (vs), 534 (w), 478 (m), 434 (m), 409 cm^{-1} (m); ^{1}H NMR (300 MHz, $CDCl_3$, 20°C, TMS): δ=13.38 (s br., 3H; NH), 2.11 ppm (s, 45H; C_5Me_5); ^{13}C{^{1}H} NMR (75 MHz, $CDCl_3$, 20°C, TMS): δ=121.2 (C_5Me_5), 12.5 ppm (C_5Me_5); elemental analysis calcd (%) for $C_{30}H_{48}I_2N_4SrTi_3$: C 37.94, H 5.09, N 5.90; found: C 39.47, H 5.05, N 5.47.

Synthesis of [Cl$_2$Sn{(μ_3-NH)$_3$Ti$_3$(η^5-C_5Me_5)$_3$(μ_3-N)}] (10): In a fashion similar to the preparation of **5**, **1** (0.50 g, 0.82 mmol) and $SnCl_2$ (0.129 g, 0.68 mmol) were allowed to react in toluene (40 mL) for 24 h to afford **10** as an orange crystalline solid (0.36 g, 67%). IR (KBr): $\tilde{\nu}$=3343 (m), 3302 (m), 2911 (s), 2858 (m), 1488 (m), 1427 (m), 1378 (s), 1067 (w), 1024 (m), 745 (s), 655 (vs), 525 (m), 474 (m), 426 cm^{-1} (m); ^{1}H NMR (300 MHz, $CDCl_3$, 20°C, TMS): δ=12.15 (s br., 3H; NH), 2.10 ppm (s, 45H; C_5Me_5); ^{13}C{^{1}H} NMR (75 MHz, $CDCl_3$, 20°C, TMS): δ=122.0 (C_5Me_5), 12.2 ppm (C_5Me_5); elemental analysis calcd (%) for $C_{30}H_{48}Cl_2N_4SnTi_3$: C 45.16, H 6.06, N 7.02; found: C 45.14, H 6.09, N 6.76.

Synthesis of [Cl$_2$Pb{(μ_3-NH)$_3$Ti$_3$(η^5-C_5Me_5)$_3$(μ_3-N)}] (11): In a fashion similar to the preparation of **5**, **1** (0.30 g, 0.49 mmol) and $PbCl_2$ (0.12 g, 0.43 mmol) were allowed to react in dichloromethane (50 mL) for 24 h to afford **11** as a yellow solid (0.23 g, 60%). IR (KBr): $\tilde{\nu}$=3301 (m), 2907 (s), 2857 (m), 1491 (m), 1429 (m), 1378 (m), 1261 (w), 1067 (w), 1027 (m), 773 (s), 729 (s), 663 (vs), 549 (w), 529 (m), 477 (m), 430 cm^{-1} (m); ^{1}H NMR (300 MHz, $CDCl_3$, 20°C, TMS): δ=12.72 (s br., 3H; NH), 2.11 ppm (s, 45H; C_5Me_5); ^{13}C{^{1}H} NMR (75 MHz, $CDCl_3$, 20°C, TMS): δ=121.7 (C_5Me_5), 12.1 ppm (C_5Me_5); elemental analysis calcd (%) for

$C_{30}H_{48}Cl_2N_4PbTi_3$: C 40.65, H 5.46, N 6.32; found: C 41.87, H 5.57, N 5.24.

Synthesis of [$I_2Sn\{(\mu_3\text{-}NH)_3Ti_3(\eta^5\text{-}C_5Me_5)_3(\mu_3\text{-}N)\}$] (12): In a fashion similar to the preparation of **9**, **1** (0.30 g, 0.49 mmol) and SnI_2 (0.18 g, 0.48 mmol) were allowed to reacted in toluene (30 mL) for 24 h to afford **12** as brown crystals (0.38 g, 81 %). IR (KBr): $\tilde{\nu}$= 3286 (m), 2910 (s), 1488 (w), 1426 (m), 1380 (s), 1027 (m), 765 (s), 735 (m), 698 (w), 654 (vs), 532 (m), 479 (m), 437 (m), 414 cm^{-1} (m); ^1H NMR (300 MHz, $CDCl_3$, 20 °C, TMS): δ = 11.59 (s br., 3H; NH), 2.21 ppm (s, 45H; C_5Me_5); $^{13}C\{^1H\}$ NMR (75 MHz, $CDCl_3$, 20 °C, TMS): δ = 124.5 (C_5Me_5), 12.5 ppm (C_5Me_5); elemental analysis calcd (%) for $C_{30}H_{48}I_2N_4SnTi_3$: C 36.74, H 4.93, N 5.71; found: C 36.63, H 4.84, N 4.05.

Reaction of 10 with MeI: A 5-mm valved NMR tube was charged with **10** (10 mg, 0.013 mmol), MeI (11 mg, 0.08 mmol), and [D_6]benzene (1.00 mL). The course of the reaction was monitored by ^1H NMR spectroscopy. After the mixture had been heated at 60 °C for six days, a good portion of dark brown crystals were grown at the bottom of the tube. The crystals were isolated and identified as $[\{ISn(\mu_3\text{-}NH)_3Ti_3(\eta^5\text{-}C_5Me_5)_3(\mu_3\text{-}N)\}_2(\mu\text{-}I)_2]\cdot C_6D_6$ (7 mg, 54 %) by X-ray crystallography, and analytical and spectroscopic data. IR (KBr): $\tilde{\nu}$ = 3286 (m), 2909 (s), 2852 (w), 1484 (w), 1426 (m), 1380 (s), 1261 (w), 1099 (w), 1070 (w), 1026 (m), 764 (vs), 709 (w), 653 (vs), 532 (m), 505 (m), 478 (m), 437 (m), 413 cm^{-1} (m); ^1H NMR (300 MHz, $CDCl_3$, 20 °C, TMS): δ = 11.69 (s br., 3H; NH), 2.19 ppm (s, 45H; C_5Me_5); $^{13}C\{^1H\}$ NMR (75 MHz, $CDCl_3$, 20 °C, TMS): δ = 124.5 (C_5Me_5), 12.5 ppm (C_5Me_5); MS (EI, 70 eV): *m*/*z* (%): 852 (1) $[ISn(\mathbf{1})]^+$, 716 (1) $[ISn(\mathbf{1})-C_5Me_5H]^+$, 247 (39) $[SnI]^+$, 119 (100) $[Sn]^+$, 84 (100) $[C_6D_6]^+$; elemental analysis calcd (%) for $C_{66}H_{96}D_6I_4N_8Sn_2Ti_6$: C 38.75, H 5.02, N 5.48; found: C 39.54, H 4.82, N 4.98.

Synthesis of [$I_3In\{(\mu_3\text{-}NH)_3Ti_3(\eta^5\text{-}C_5Me_5)_3(\mu_3\text{-}N)\}$] (13): A solution of InI_3 (0.163 g, 0.33 mmol) in toluene (30 mL) was added dropwise to **1** (0.20 g, 0.33 mmol) in toluene (20 mL). The resultant solution was immediately filtered and kept at room temperature for three days. After that time, a fraction of brown crystals of **13** was collected by filtration. The remaining solution was stirred for 1 h to give a second crop of **13**. The combined yield for **13** was 0.24 g (80 %). IR (KBr): $\tilde{\nu}$ = 3358 (m), 3279 (w), 2910 (s), 2857 (m), 1488 (m), 1426 (s), 1378 (s), 1023 (m), 904 (m), 750 (s), 708 (m), 663 (vs), 645 (s), 601 (s), 525 (m), 473 (m), 431 cm^{-1} (m); ^1H NMR (300 MHz, $CDCl_3$, 20 °C, TMS): δ = 11.40 (s br., 3H; NH), 2.11 ppm (s, 45H; C_5Me_5); $^{13}C\{^1H\}$ NMR (75 MHz, $CDCl_3$, 20 °C, TMS): δ = 122.1 (C_5Me_5), 12.4 ppm (C_5Me_5); MS (EI, 70 eV): *m*/*z* (%): 970 (1) $[M-C_5Me_4CH_2]^+$, 496 (14) $[InI_3]^+$, 369 (54) $[InI_2]^+$, 242 (84) $[InI]^+$; elemental analysis calcd (%) for $C_{30}H_{48}I_3InN_4Ti_3$(%): C 32.64, H 4.38, N 5.08; found: C 33.06, H 4.45, N 4.82.

X-ray structure determination of complexes 10, 12, and 13: X-ray crystals of **13** were grown as described in the Experimental Section. Crystals were mounted in a glass capillary in a random orientation and transferred to an Enraf-Nonius CAD4 diffractometer for characterization and data collection at room temperature. Crystals of complexes **10** and **12** were grown as described in the Experimental Section, removed from the Schlenk flasks and covered with a layer of a viscous perfluoropolyether (FomblinY). A suitable crystal was selected with the aid of a microscope, attached to a glass fiber, and immediately placed in the low-temperature nitrogen stream of the diffractometer. The intensity data sets were collected at 100 K on a Bruker-Nonius KappaCCD diffractometer equipped with an Oxford Cryostream 700 unit. Crystallographic data for all the complexes are presented in Table 5.

The structures were solved, by using the WINGX package,[31] by Patterson (**10**) or direct methods (**12** and **13**) (SHELXS-97), and refined by least-squares against F^2 (SHELXL-97).[32]

Two independent molecules of complex **10** crystallized in the triclinic space group $P\bar{1}$. The tin atoms presented disorder and were each refined at two sites with occupancies of 85 % and 15 %. All non-hydrogen atoms of **10** were anisotropically refined. The hydrogen atoms of the pentamethylcyclopentadienyl rings were included, positioned geometrically and refined by using a riding model, and all the imido-hydrogen atoms were located in the Fourier difference map and isotropically refined.

Complex **12** crystallized in a dimeric form with one molecule of [D_6]benzene. All the non-hydrogen atoms were anisotropically refined. Only the imido-hydrogen atoms were directly located in the Fourier difference map and isotropically refined, the pentamethylcyclopentadienyl hydrogen atoms were included, positioned geometrically, and refined by using a riding model.

Medium-quality crystals of **13** were crystallized in toluene, in the noncentrosymmetric space group $P2_1$. All the non-hydrogen atoms were refined anisotropically and all the hydrogen atoms were included, geometrically positioned, and refined by using a riding model. The highest peak (2.013 e$Å^{-3}$) and hole (−2.058 e$Å^{-3}$) found in the difference Fourier map are located close to In1 (0.78 and 1.69 Å, respectively).

Table 5. Experimental data for the X-ray diffraction studies on compounds **10, 12** and **13**.

	10	**12**	**13**
empirical formula	$C_{30}H_{48}Cl_2N_4SnTi_3$	$C_{66}H_{102}I_4N_8Sn_2Ti_6$	$C_{30}H_{48}I_3InN_4Ti_3$
M_r	798.01	2039.80	1103.94
T [K]	100(2)	150(2)	293(2)
λ [Å]	0.71073	0.71073	0.71073
crystal system	triclinic	orthorhombic	monoclinic
space group	$P\bar{1}$	*Pnnm*	$P2_1$
a [Å]; α [°]	12.237(2);100.82(1)	14.947(1)	10.679(5)
b [Å];β [°]	13.186(3);103.01(1)	16.508(3)	17.031(5);104.26(1)
c [Å];γ [°]	22.489(2);96.41(1)	16.117(3)	11.250(5)
V[Å^3]	3427.5(9)	3976.8(11)	1983.0(14)
Z	4	2	2
ρ_{calcd} [g cm^{-3}]	1.546	1.704	1.849
$\mu_{MoK\alpha}$ [mm^{-1}]	1.575	2.780	3.515
F(000)	1624	1996	1060
crystal size [mm]	0.51 × 0.16 × 0.15	0.46 × 0.46 × 0.27	0.35 × 0.30 × 0.25
θ range [°]	5.01 to 27.50	3.09 to 27.52	3.03 to 24.97
index ranges	$-15 \le h \le 15$, $-17 \le k \le 17$, $-29 \le l \le 29$	$-19 \le h \le 19$, $-21 \le k \le 21$, $-20 \le l \le 20$	$0 \le h \le 12$, $0 \le k \le 20$, $-13 \le l \le 12$
reflections collected	120972	81084	3806
unique data	15622[R_{int} = 0.166]	4714 [R_{int} = 0.103]	3609[R_{int} = 0.032]
obsd data [$I > 2\sigma(I)$]	12021	3842	3060
GOF on F^2	1.057	1.092	1.141
final *R* indices [$I > 2\sigma(I)$]	*R*1 = 0.048, *wR*2 = 0.116	*R*1 = 0.029, *wR*2 = 0.062	*R*1 = 0.082, *wR*2 = 0.236
R indices (all data)	*R*1 = 0.071, *wR*2 = 0.128	*R*1 = 0.045, *wR*2 = 0.068	*R*1 = 0.098, *wR*2 = 0.253
largest diff. peak/hole [e$Å^{-3}$]	1.932/−1.619	0.860/−1.145	2.013/−2.058

CCDC-240132–CCDC-240134 contain the supplementary crystallographic data for this paper. These data can be obtained free of charge via www.ccdc.cam.ac.uk/conts/retrieving.html (or from the Cambridge Crystallographic Data Centre, 12 Union Road, Cambridge CB2 1EZ, UK (fax: (+44)1223-336-033; or deposit@ccdc.cam.uk)).

Computational details: All DFT calculations were carried out with the ADF program[33] by using triple-ζ and polarization Slater basis sets to describe the valence electrons of C and N. For titanium, a frozen core composed of the 1s, 2s, and 2p orbitals was described by double-ζ Slater functions, the 3d and 4s orbitals by triple-ζ functions, and the 4p orbital by a single orbital. Hydrogen atoms were described by triple-ζ and polarization functions. The geometries and binding energies were calculated with gradient corrections. We used the local spin density approximation, characterized by the electron-gas exchange (Xα with $\alpha = 2/3$) together with Vosko–Wilk–Nusair parametrization[34] for correlation. Becke's nonlocal corrections[35] to the exchange energy and Perdew's nonlocal corrections[36] to the correlation energy were added. Quasirelativistic corrections were employed by using the Pauli formalism with corrected core potentials. The quasirelativistic frozen core shells were generated with the auxiliary program DIRAC.[33]

Acknowledgement

This work was supported by the Spanish MCYT (BQU2001–1499 and BQU2002–04110-C02–01), DGICAM (07N/0091/2002), CIRIT of Generalitat de Catalunya (SGR01–00315), and the Universidad de Alcalá.

[1] H. W. Roesky, Y. Bai, M. Noltemeyer, *Angew. Chem.* **1989**, *101*, 788–789; *Angew. Chem. Int. Ed. Engl.* **1989**, *28*, 754–755.
[2] A. Abarca, P. Gómez-Sal, A. Martín, M. Mena, J. M. Poblet, C. Yélamos, *Inorg. Chem.* **2000**, *39*, 642–651.
[3] A. Abarca, M. Galakhov, P. Gómez-Sal, A. Martín, M. Mena, J. M. Poblet, C. Santamaría, J. P. Sarasa, *Angew. Chem.* **2000**, *112*, 544–547; *Angew. Chem. Int. Ed.* **2000**, *39*, 534–537.
[4] A. Abarca, A. Martín, M. Mena, C. Yélamos, *Angew. Chem.* **2000**, *112*, 3602–3605; *Angew. Chem. Int. Ed.* **2000**, *39*, 3460–3463.
[5] M. García-Castro, A. Martín, M. Mena, A. Pérez-Redondo, C. Yélamos, *Chem. Eur. J.* **2001**, *7*, 647–651.
[6] K. Freitag, J. Gracia, A. Martín, M. Mena, J. M. Poblet, J. P. Sarasa, C. Yélamos, *Chem. Eur. J.* **2001**, *7*, 3644–3651.
[7] A. Martín, M. Mena, A. Pérez-Redondo, C. Yélamos, *Organometallics* **2002**, *21*, 3308–3310.
[8] A. Abarca, M. V. Galakhov, J. Gracia, A. Martín, M. Mena, J. M. Poblet, J. P. Sarasa, C. Yélamos, *Chem. Eur. J.* **2003**, *9*, 2337–2346.
[9] A. Martín, M. Mena, A. Pérez-Redondo, C. Yélamos, *Inorg. Chem.* **2004**, *43*, 2491–2498.
[10] M. García-Castro, A. Martín, M. Mena, C. Yélamos, *Organometallics* **2004**, *23*,1496–1500.
[11] For alkali-metal halide complexes, see: a) F. R. Mair, R. Snaith in *Encyclopedia of Inorganic Chemistry*, *Vol. 1* (Ed.: R. B. King), Willey, **1994**, pp. 35–54, and references therein; b) T. P. Hanusa in *Comprehensive Coordination Chemistry II Vol. 2* (Eds.: G. F. R. Parkin, J. A. McCleverty, T. J. Meyer), Elsevier, **2004**, pp. 1–92, and references therein.
[12] For examples of entrapment of MX_n molecules generated in situ by donor ligands, see: a) S. R. Hall, C. L. Raston, B. W. Skelton, A. H. White, *Inorg. Chem.* **1983**, *22*, 4070–4073; b) C. L. Raston, B. W. Skelton, C. R. Whitaker, A. H. White, *J. Chem. Soc. Dalton Trans.* **1988**, 987–990; c) F. S. Mair, W. Clegg, P. A. O'Neil, *J. Am. Chem. Soc.* **1993**, *115*, 3388–3389; d) A. D. Bond, E. L. Doyle, S. J. Kidd, A. D. Woods, D. S. Wright, *Chem. Commun.* **2001**, 777–778; e) T. Chivers, A. Downard, M. Parvez, G. Schatte, *Inorg. Chem.* **2001**, *40*, 1975–1977; f) P. Wei, D. W. Stephan, *Organometallics* **2003**, *22*, 601–604.
[13] For examples of entrapment of MX_n molecules by ligands in *direct reactions*, see: a) R. E. Mulvey, W. Clegg, D. Barr, R. Snaith, *Polyhedron* **1986**, *5*, 2109–2111; b) C. L. Raston, C. R. Whitaker, A. H. White, *J. Chem. Soc. Dalton Trans.* **1988**, 991–995; c) C. L. Raston, C. R. Whitaker, A. H. White, *Inorg. Chem.* **1989**, *28*, 163–165; d) T. Chivers, M. Parvez, G. Schatte, *Inorg. Chem.* **2001**, *40*, 540–545; e) S. H. Oakley, D. B. Soria, M. P. Coles, P. B. Hitchcock, *Dalton Trans.* **2004**, 537–546.
[14] a) D. Barr, W. Clegg, R. E. Mulvey, R. Snaith, *J. Chem. Soc, Chem. Commun.* **1984**, 79–80; b) D. Barr, R. Snaith, D. S. Wright, R. E. Mulvey, K. Wade, *J. Am. Chem. Soc.* **1987**, *109*, 7891–7893; c) D. Barr, M. J. Doyle, R. E. Mulvey, P. R. Raithby, D. Redd, R. Snaith, D. S. Wright, *J. Chem. Soc. Chem. Commun.* **1989**, 318–319; d) D. Barr, A. T. Brooker, M. J. Doyle, S. R. Drake, P. R. Raithby, R. Snaith, D. S. Wright, *J. Chem. Soc. Chem. Commun.* **1989**, 893–895.
[15] NMR data for $[ClIn\{(\mu_3\text{-}NH)_3Ti_3(\eta^5\text{-}C_5Me_5)_3(\mu_3\text{-}N)\}]$: ^{1}H NMR (300 MHz, C_6D_6, 20 °C, TMS): $\delta = 13.60$ (s br., 3H; NH), 2.00 ppm (s, 45H; C_5Me_5); $^{13}C\{^1H\}$ NMR (75 MHz, C_6D_6, 20 °C, TMS): $\delta =$ 117.6 (C_5Me_5), 11.9 ppm ($C_5\mathit{Me}_5$).
[16] F. García, A. D. Hopkins, S. M. Humphrey, M. McPartlin, M. C. Rogers, D. S. Wright, *J. Chem. Soc, Dalton Trans.* **2004**, 361–362.
[17] The atom···atom long-distance interactions or angles around them have been calculated with PLATON: A. L. Spek, *Acta Crystallogr. Sect. A* **1990**, *46*, C-34.
[18] Similar long-distance Sn···Sn interactions can be calculated with the program Conquest for: a) M. Veith, M. Jarczyk, V. Huch, *Chem. Ber.* **1988**, *121*, 347–355; b) A. G. Kolchinski, N. W. Alcock, *J. Org. Chem.* **1998**, *63*, 4515–4517; c) N. Kuhn, R. Fawzi, H. Kotowski, M. Steimann, *Z. Kristallogr. New Cryst. Struct.* **1998**, *213*, 435–436.
[19] Conquest: New software for searching the Cambridge Structural Database and visualizing crystal structures: I. J. Bruno, J. C. Cole, P. R. Edgington, M. Kessler, C. F. Macrae, P. McCabe, J. Pearson, R. Taylor, *Acta Crystallogr. Sect. B* **2002**, *58*, 389–397.
[20] a) R. E. Allan, M. A. Beswick, N. Feeder, M. Kranz, M. E. G. Mosquera, P. R. Raithby, A. E. H. Wheatley, D. S. Wright, *Inorg. Chem.* **1998**, *37*, 2602–2604; b) S. Suh, D. M. Hoffman, *Inorg. Chem.* **1996**, *35*, 6164–6169.
[21] C. Lode, H. Krautscheid, *Z. Anorg. Allg. Chem.* **2001**, *627*, 841–846.
[22] a) N. H. Greenwood, A. Earnshow, *Chemistry of the elements.* 2 ed. Butterworth Heinemann, Oxford, **1998**, p. 60; b) C. J. Horn, A. J. Blake, N. R. Champness, A. Garau, V. Lippolis, C. Wilson, M. Schröder, *Chem. Commun.* **2003**, 312–313.
[23] M. A. Brown, D. G. Tuck, *Inorg. Chim. Acta* **1996**, *247*, 135–138, and references therein.
[24] For some examples of In–N dative bonds in complexes bearing InI fragments, see: a) M. A. Khan, C. Peppe, D. G. Tuck, *J. Organomet. Chem.* **1985**, *280*, 17–25; b) R. A. Fischer, S. Nlate, H. Hoffmann, E. Herdtweck, J. Blumel, *Organometallics* **1996**, *15*, 5746–5752.
[25] For some examples of complexes bearing InI fragments, see: a) J. Janczak, R. Kubiak, *Inorg. Chim. Acta* **1999**, *288*, 174–180; b) T. Grabowy, K. Merzweiler, *Z. Anorg. Allg. Chem.* **2000**, *626*, 736–740.
[26] G. R. Willey, D. R. Aris, J. V. Haslop, W. Errington, *Polyhedron* **2001**, *20*, 423–429.
[27] D. C. Bradley, D. M. Frigo, I. S. Harding, M. B. Hursthouse, M. Motevalli, *J. Chem. Soc. Chem. Commun.* **1992**, 577–578.
[28] C. C. Pye, T. Ziegler, *Theor. Chem. Acc.* **1999**, *101*, 396–408.
[29] R. T. Sanderson , *Chemical Bonds and Bond Energy*, 2nd ed., Academic Press, N. York, **1976**.
[30] *CRC Handbook of Chemistry and Physics. 2002–2003: A Ready-Reference Book of Chemical and Physical Data (CRC Handbook of Chemistry and Physics*), 83rd ed, (Ed.: D. R. Lide), CRC Press, Boca Raton, Florida, USA, **2002**.
[31] L. J. Farrugia. WinGX - A Windows Program for Crystal Structure Analysis, University of Glasgow, Glasgow, **1998**.
[32] G. M. Sheldrick, SHELX97, Program for Crystal Structure Analysis (Release 97–2). Universität Göttingen, Germany, **1998**.
[33] a) ADF 2000.01, Department of Theoretical Chemistry, Vrije Universiteit, Amsterdam; b) E. J. Baerens, D. E. Ellis, P. Ros, *Chem. Phys.* **1973**, *2*, 41–51; c) L. Versluis, T. Ziegler, *J. Chem. Phys.* **1988**, *88*, 322–328; d) G. Te Velde, E. J. Baerens, *J. Comput. Phys.* **1992**,

99, 84–98; e) C. Fonseca Guerra, J. G. Snijders, G. Te Velde, E. J. Baerens, *Theor. Chem. Acc.* **1998**, *99*, 391–403.
[34] S. H. Vosko, L. Wilk, M. Nusair, *Can. J. Phys.* **1980**, *58*, 1200–1211.
[35] a) A. D. Becke, *J. Chem. Phys.* **1986**, *84*, 4524–4529; b) A. D. Becke, *Phys. Rev. A* **1988**, *38*, 3098–3100.
[36] a) J. P. Perdew, *Phys. Rev. B* **1986**, *33*, 8822–8824; b) J. P. Perdew, *Phys. Rev. B* **1986**, *34*, 7406–7406.

Received: June 3, 2004
Published online: December 21, 2004

